ISSN 0023-1584, Kinetics and Catalysis, 2011, Vol. 52, No. 4, pp. 620–628. © Pleiades Publishing, Ltd., 2011.
Original Russian Text © D.S. Ovoshchnikov, I.S. Glaznev, Yu.I. Aristov, 2011, published in Kinetika i Kataliz, 2011, Vol. 52, No. 4, pp. 630–639.

# Water Sorption by the Calcium Chloride/Silica Gel Composite: The Accelerating Effect of the Salt Solution Present in the Pores

**D. S. Ovoshchnikov, I. S. Glaznev, and Yu. I. Aristov***

*Boreskov Institute of Catalysis, Siberian Branch, Russian Academy of Sciences, Novosibirsk, 630090 Russia*

**e-mail aristov@catalysis.ru*

Received April 30, 2010

**Abstract**—The kinetics of isothermal water sorption by the $CaCl_2$/silica gel composite initiated by a small stepwise pressure rise over the sample has been investigated at a constant underlying plate temperature of 35°C. The initial portion of the kinetic curves is consistent with Fick's diffusion model: the amount of sorbed water increases in proportion to the square root of the sorption time. This makes it possible to determine the effective diffusivity of water ($D_{eff}$). At small amounts of sorbed water ($w < 0.19$ g/g), $D_{eff}$ changes slightly. The diffusivity of water in the composite pores ($D$) calculated for the same conditions is close to the Knudsen diffusivity of water vapor in mesopores. The $D_{eff}$ value grows with an increasing water content of the composite; that is, sorbed water accelerates water transport in the pores. This is likely due to the appearance of an extra diffusion channel, namely, diffusion through the aqueous solution of the salt, whose formation begins on the silica gel surface at $w > 0.1$ g/g. The contribution from this channel increases markedly when the amount of adsorbed water is above 0.25 g/g. This can be explained by the formation of the "connected" phase of the solution in the pores.

**DOI:** 10.1134/S0023158411040124

Water adsorption by porous materials is a component of many important processes, such as gas and liquid drying, thermal energy conversion and storage, and humidity control [1–4]. In order to raise the efficiency of an adsorbent, it is necessary to have information concerning its dynamic behavior in wide temperature and water vapor pressure ranges. Of particular interest in this context are new classes of adsorbents, including salt-in-porous-matrix composites [5, 6]. A specific feature of these composites is that water is mainly sorbed by the disperse salt. This yields first a hydrate and then an aqueous solution of the salt in the pores of the matrix [6, 7]. The formation of a solution phase in the pores of the composite can complicate the water sorption kinetics relative to the kinetics of water adsorption on conventional, single-component adsorbents [8]. The interaction between water and the surface of the latter proceeds rapidly, and the adsorption rate is usually limited by the transport of water vapor inside the granule or by the dissipation of the heat of adsorption [1, 9].

A classical method of measuring the diffusivity is the isothermal differential method [9], in which the driving force of adsorption is a small deviation of the water vapor pressure from its equilibrium value. The existence of a simple mathematical model of sorption (see Appendix A) makes it possible to determine macroscopic parameters characterizing the adsorption kinetics [10, 11], such as the effective diffusivity of water, $D_{eff}$. The isothermal differential method that was used in an earlier work [12] to investigate the kinetics of water vapor adsorption by the $CaCl_2$/silica gel composite in the temperature range of $T = 33$–69°C and pressure range of $P_{H_2O} = 8$–70 mbar. Measurements were carried out by the thermogravimetric method. The granule size was varied between 0.355 and 1.4 mm. It was demonstrated that, in the initial portion of the kinetic curve, the amount of water adsorbed ($\Delta m$) is proportional to the square root of the adsorption time $t$, which is in agreement with Fick's diffusion mechanism. From the slope of the curve in the $\Delta m$–$t^{1/2}$ coordinates, the effective diffusivity $D_{eff}$ was derived, which turned out to be independent of the mean granule radius $r_c$ for $r_c \geq 0.355$ mm. For smaller granules, the adsorption rate increases less rapidly than it would do if it were proportional to $r_c^{-2}$. This is likely due to the effect of the thermal effects associated with water sorption. The effective diffusivity of water vapor in the pores was determined to be $D = (0.46 \pm 0.12) \times 10^{-6}$ m$^2$/s, approximately 10 times smaller than the Knudsen diffusivity of water calculated for a single cylindrical pore whose size is equal to the mean pore size of the composite.

The mathematical model used in that work for kinetic analysis allowed for water diffusion only in the gas phase. It was assumed that the spatial configuration of this phase does not vary during adsorption, being independent of the amount of adsorbed water. In salt-in-porous-matrix adsorbents, the salt solution gradually fills the matrix pores as water is sorbed [5, 6].

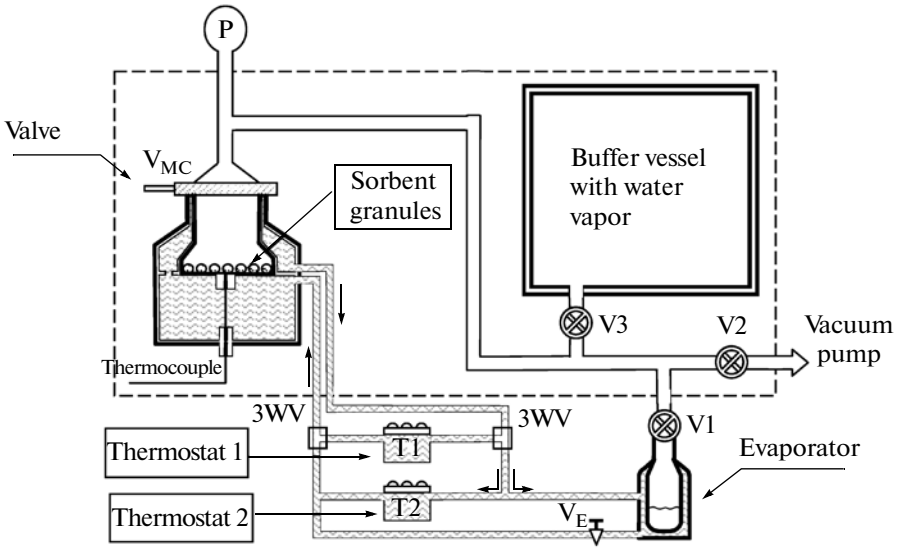


**Fig. 1.** Setup for investigation of water sorption kinetics and equilibrium.

As a consequence, the space available for vapor diffusion decreases gradually and the solution phase appears on the matrix surface, and this phase can also contribute to the transport of water molecules. These effects are analyzed in the present study. A specific feature of our experiments was that we used a new variant of the isothermal differential method, in which sorbent granules were placed on a massive isothermal metallic plate. We believe that this placement of the adsorbent reduces the effect of the heat of sorption and ensures more isothermal conditions for the adsorbent granules.

## EXPERIMENTAL

### *Sorbent Preparation*

The initial silica gel granules (Aldrich, mean pore size of 9 nm, specific surface area of 390 $m^2/g$, pore volume of 0.93 $cm^3/g$) were ground, and the 0.4–0.5 mm size fraction was taken. This fraction was air-dried at 200°C and was cooled to room temperature in a desiccator. The composite sorbent was prepared by incipient-wetness impregnation of the dry granules (initial weight $m_{dry}$) with a saturated calcium chloride solution. The aqueous solutions of calcium chloride were prepared from $CaCl_2 \cdot 6H_2O$ (Reakhim) and distilled water. The impregnated granules were dried at 200°C in air to constant weight ($m_{comp}$). Their salt content, calculated as $g = (m_{comp} - m_{dry})/m_{comp}$, was 21 wt %. The fraction of the pore volume occupied by the salt, its hydrates, and/or its aqueous solution (ν) was calculated as $\nu = \frac{V_f}{V_p} = \frac{m}{\rho V_p}$, where $V_f$ is the volume occupied by the salt hydrate and/or solution in the pores, $V_p$ is the pore volume of the silica gel, $m$ is the weight of the hydrate (solution), and ρ is the hydrate (solution) density.

### *Kinetic Study of Water Sorption*

The water sorption kinetics was studied at 35°C in the relative water vapor pressure range of $P/P_0 = 0$–0.85 using the isothermal differential method. The adsorbent granules as a single layer were placed on a massive metallic plate (Fig. 1). The plate was maintained at a constant temperature with a flowing heat carrier (water). The other elements of the setup, including the buffer vessel with water vapor, were maintained at the same temperature.

Water sorption (desorption) was initiated by producing a small stepwise deviation of the pressure in the system from the equilibrium pressure. Experiments were performed as follows. The valve $V_{MC}$ (Fig. 1) was closed, and the buffer vessel, whose volume was $V_{buf} = 30.5 \times 10^{-3}$ $m^3$, was filled with water vapor up to a preset pressure $P_1$, which was produced by maintaining the evaporator at a preset temperature $T_1$. As this was done, the valves $V_1$ and $V_3$ were open and the valve $V_2$ was closed. After the initial pressure $P_1$ was established (which took approximately 1 h), the valve $V_1$ was closed, the valve $V_{MC}$ was opened, and the measurement cell ($V_{meas} = 0.14 \times 10^{-3}$ $m^3$) was thus connected to the buffer vessel. As a result, the vapor pressure in the cell increased quickly to $P_1^0 = P_1 V/(V_{buf} + V_{meas})$. This initiated water sorption, which caused a decrease in the pressure over the sample in time ($P(t)$). The current amount of sorbed water was calculated as $m_t =$

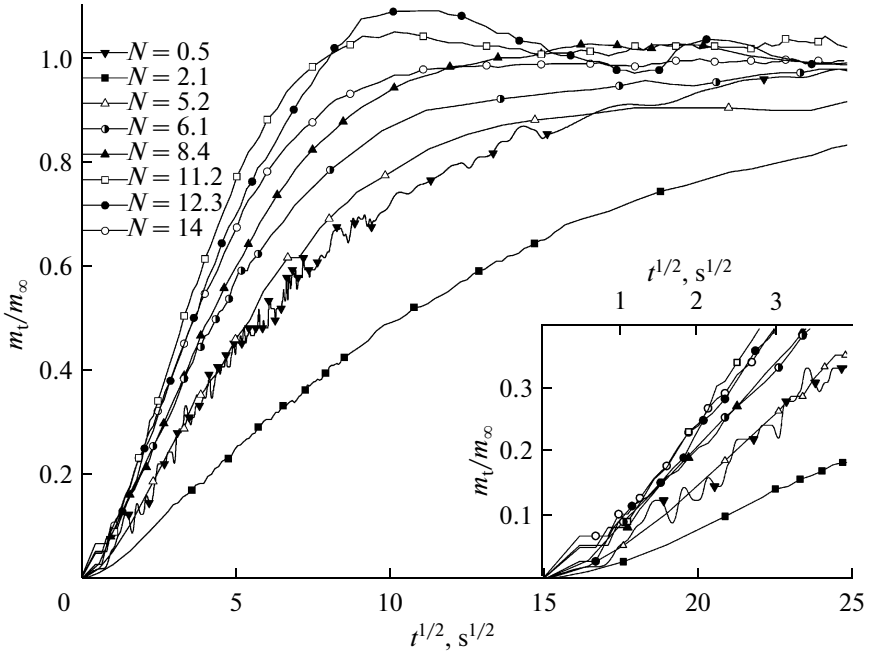


**Fig. 2.** Water vapor sorption curves for the $CaCl_2$/silica gel composite at $T = 35°C$ and different final water content ($N$) values. The inset shows the initial portions of the curves on an enlarged scale.

$M(P_1^0 - P(t))(V_{buf} + V_{meas})/RT$, where $M$ is the molar mass of water and $R$ is the gas constant. The equilibrium specific amount of sorbed water ($w$) at the ultimate pressure $P_1^* = P(t \longrightarrow \infty)$ and temperature $T_1$ was calculated as $w(P_1^*, T_1) = m_\infty/m_{comp}$. The amount of sorbed water was also expressed in terms of the number of moles of water taken up by 1 mol of the salt: $N = \dfrac{w\mathrm{M}}{\mathrm{M}_{CaCl_2}g}$, where $\mathrm{M}_{CaCl_2} = 110.99$ g/mol is the molar mass of calcium chloride. Next, the valve $V_{MC}$ was closed, the evaporator temperature was raised to $T_2$, and the measurement cycle was repeated with a vapor pressure of $P_2 > P_1$ in the buffer vessel, and so on. The vapor pressure in the system was measured with an MKS Baratron® Type 626A precision pressure transducer (designated P in Fig. 1) with an accuracy of ±0.2%.

## RESULTS AND DISCUSSION

### *Water Sorption Kinetics*

The dimensionless quantity $m_t/m_\infty$ as a function of the square root of the sorption time $t$ at $T = 35°C$ and selected ultimate amounts of sorbed water ($N$) is plotted in Fig. 2. At the early stages of sorption, $m_t$ is proportional to $t^{1/2}$, and then it plateaus. This is in qualitative agreement with Fick's diffusion model. For $N =$ 11.2 and 12.3 ($w = 0.392$ and 0.420, respectively), the amount sorbed at $t \approx 100$ s exceeds the equilibrium value by 5–10%. The cause of this overequilibrium sorption remains unclear. On the whole, the initial sorption rate increases with an increasing amount of already sorbed water (Fig. 2), but some deviations from this rule are observed, however. For example, the slowest sorption is observed for $N = 2.1$ ($w = 0.073$); the most rapid sorption, for $N = 11.2$.

A qualitative analysis of the sorption kinetics at small amounts of adsorbed water can be carried out using the well-known model in which the interaction between water and the surface is assumed to be rapid and the overall process rate is determined by the rate of water diffusion in the pore space [9–11]. At small $t$ values, the exact solution for this model (Appendix A) is given by the simple expression

$$\frac{m_t}{m_\infty} = \frac{1}{1-\Lambda}\frac{6}{\sqrt{\pi}}\sqrt{\frac{D_{eff}t}{r_c^2}} \propto \sqrt{t}, \qquad (1)$$

where $r_c$ is the granule radius and $\Lambda = \dfrac{\Delta P_a}{\Delta P_0}$ is the ratio of the adsorption-induced change in the water vapor pressure over the sample ($\Delta P_a$) to the initial pressure jump ($\Delta P_0$). The $D_{eff}$ values derived from the slopes of the curves in the $\dfrac{m_t}{m_\infty} \sim t^{1/2}$ coordinates at small $t$ values are listed in the table along with the calculated diffusivitys of water in the pores, $D = D_{eff}\dfrac{\varepsilon + (1-\varepsilon)K}{\varepsilon}$. Thus, in order to calculate $D$, it is necessary to determine the local slope of the sorption isotherm ($K$) and the porosity of the adsorbent granules ($\varepsilon$). The slope $K$ was

Some parameters of water sorption by the $CaCl_2$/silica gel composite and quantities used for their calculation

| $P_0$, mbar | $P_{fin}$, mbar | $\Lambda$ | $\varepsilon$ | $\nu$ | $w$, g/g | $N$ | $D_{eff} \times 10^{11}$, $m^2/g$ | $D \times 10^6$, $m^2/g$ |
|---|---|---|---|---|---|---|---|---|
| 0.58 | 0.44 | 0.23 | 0.587 | 0.11 | 0.017 | 0.5 | 3.1 | – |
| 0.96 | 1.48 | 0.5 | 0.549 | 0.15 | 0.073 | 2.1 | 0.5 | – |
| 4.66 | 4.96 | 0.11 | 0.517 | 0.22 | 0.115 | 3.3 | 4.6 | 1.2 |
| 5.30 | 5.49 | 0.23 | 0.500 | 0.24 | 0.136 | 3.9 | 3.0 | 1.6 |
| 5.95 | 6.19 | 0.27 | 0.477 | 0.25 | 0.157 | 4.5 | 3.1 | 1.7 |
| 7.00 | 7.18 | 0.14 | 0.456 | 0.27 | 0.182 | 5.2 | 4.9 | 1.9 |
| 8.70 | 8.98 | 0.15 | 0.427 | 0.31 | 0.213 | 6.1 | 6.1 | – |
| 13.40 | 14.05 | 0.11 | 0.353 | 0.41 | 0.294 | 8.4 | 8.5 | – |
| 17.31 | 17.82 | 0.12 | 0.299 | 0.50 | 0.353 | 10.1 | 12.1 | – |
| 20.60 | 20.98 | 0.10 | 0.264 | 0.58 | 0.392 | 11.2 | 15.2 | – |
| 23.62 | 23.97 | 0.11 | 0.230 | 0.65 | 0.420 | 12.3 | 12.8 | – |
| 27.75 | 28.30 | 0.12 | 0.173 | 0.75 | 0.490 | 14.0 | 11.3 | – |

Note: $P_0$ is the initial pressure, $P_{fin}$ is the final pressure, $\Lambda$ is a calculated parameter, $\varepsilon$ is porosity, $\nu$ is the fraction of pore volume filled by the salt, $w$ and $N$ designate the final amount of sorbed water, $D_{eff}$ is the effective diffusivity, and $D$ is the diffusivity of water in the pores.

determined by numerical differentiation of the water adsorption isotherm at $T = 35°C$ (Appendix B). The error of this procedure was large, particularly at small amounts sorbed. For this reason, $D$ was calculated at $N \geq 3.3$ (table).

In the calculation of the porosity $\varepsilon$, we took into account the decrease in the pore volume of the initial silica gel due to the following: part of the pores is occupied by the introduced salt and, as a consequence, $\varepsilon = 0.59$, while the porosity of the initial silica gel is 0.67; water sorption in the pores initially yields solid hydrates with $N = 1/3$, 1, and 2 [7, 13], whose molar volume is larger than that of the anhydrous salt [14], and then an aqueous solution of the salt, which results in a progressive decrease in $\varepsilon$ during water sorption (table).

Details of the calculation of the porosity $\varepsilon$ and the water-filled pore volume fraction $\nu$ are given in Appendix B.

As was mentioned above, the model considered here is valid only for small amounts sorbed; however, it is difficult to precisely specify the limits of its applicability. For this reason, $D$ was calculated only for $N$ not larger than 5.2. At small amounts sorbed ($N < 3.9$), the diffusivity of water in the pores is $1.2 \times 10^{-6}$ $m^2/s$. This value is somewhat smaller than the Knudsen diffusivity calculated for a cylindrical pore with a radius of $r_p = 4.5$ nm at $T = 308$ K [1]: $D_{Kn} = 9700 r_p \sqrt{T/M} = 1.8 \times 10^{-6}$ $m^2/s$. This likely indicates that Knudsen diffusion makes a significant contribution to the dynamics of sorption of the first portions of water. Knowing the $D_{Kn}/D$ ratio, we determined that $\chi/\varepsilon = 1.5$, where $\chi$ is the tortuosity factor of the sorbent pores. Under the assumption that $\varepsilon = 0.52$ at small amounts sorbed, the tortuosity factor is estimated at $\chi \approx 1$, which is in agreement with the value determined for the initial silica gel by pulsed field gradient NMR ($\chi = 1.2$).

Note that the effective diffusivity of water vapor in the pores of the similar composite sorbent SWS-1L was determined earlier to be $D = (0.46 \pm 0.12) \times 10^{-6}$ $m^2/s$, 2–3 times smaller than the value obtained in this study, and this leads to a larger value of the tortuosity factor. The authors hypothesized that a possible cause of the increased tortuosity is that the salt introduced into the silica gel blocks part of its pores. Apparently, as water is being removed from the solution at the synthesis stage, part of the salt deposits in silica gel pores and blocks them. As a consequence, the initial pore connectivity deteriorates and the tortuosity factor increases. The salt distribution has not been the subject of our investigation, but an analysis made by other authors [15] demonstrated that it may depend strongly on how the matrix surface is wetted by the salt solution and on the drying conditions. The SWS-1L composite was prepared industrially according to the Russian Specifications TU 2163-026-03533913-00 [16], and the drying conditions for the batch to which the sample belonged are unknown. It is quite likely that they differ from the preparation conditions for the $CaCl_2/SiO_2$ composite examined in this work. This difference is a likely cause of the difference between the degrees of blocking and, accordingly, tortuosities of the pores of the two composites.

The underestimation of $D$ in [12] could arise from thermal effects. Water sorption in a sorbent granule is accompanied by heat evolution. When heat removal is hindered, the granule heats, and this slows down water sorption. This slowdown can hardly be avoided in thermogravimetric experiments in which a light measurement cell with a sample is suspended in a vacu-

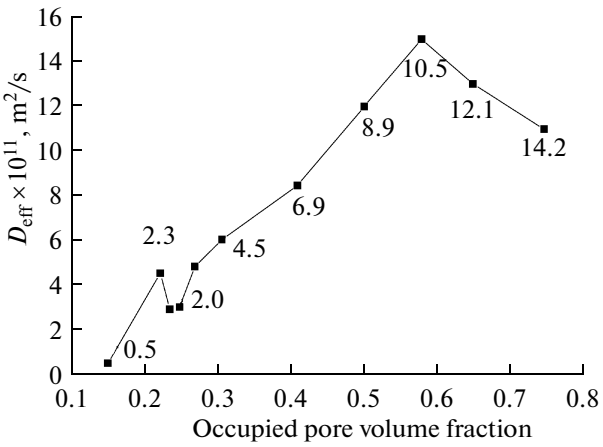


**Fig. 3.** Effective diffusivity of water vapor as a function of the occupied pore volume fraction. The numbers at the data points indicate the amount sorbed ($N$).

umized chamber and has no contact with the walls [17]. The thermal effects are commonly reduced by using a small-weight sample and by mixing it with a metal powder in order to increase the heat capacity of the measurement cell [18]. In our experiments, the adsorbent was placed on a massive metallic plate, which was maintained at constant temperature with a flowing heat carrier. With this technique, water sorption possibly took place under more isothermal conditions, thus allowing the diffusivitys and pore tortuosity to be determined more accurately. A more detailed analysis of the initial portions of the kinetic curves (inset in Fig. 2) demonstrated that, at sorption times of 2–5 s, the sorption rate is always lower than it would be in the case of isothermal diffusion. This likely indicates that thermal effects do take place even when the adsorbent is placed on an isothermal plate whose heat conductivity is many times higher than that of the adsorbent.

Thus, at comparatively small amounts of sorbed water ($N < 4$–5), the process is primarily controlled by water vapor transport in the pore space, which occurs mainly via Knudsen diffusion.

As the amount of sorbed waster increases, the water sorption rate grows (Fig. 2). For example, as $N$ increases to 5.2, the diffusivity $D$ increases almost by a factor of 1.5 (table). The $D_{eff}$ value also grows (Fig. 3). This possibly indicates the appearance of another channel for water transport in the pores. This is quite likely in view of the change in the phase composition of the system during water sorption. As was mentioned above, the first portions of water are sorbed via the reaction $CaCl_2 + N H_2O = CaCl_2 \cdot N H_2O$, which yields solid salt hydrates with $N = 1/3$, 1, and 2 [7, 13]. At later stages, the salt dihydrate adds two more water molecules, thus yielding the tetrahydrate in the pores. The melting point of this tetrahydrate in the massive state is 38.4°C [14]. When a compound is in pores, it melts below its normal melting point, so it is likely that, under our experimental conditions ($T = 35$°C), the tetrahydrate undergoes melting and, at $N > 2$, there is a salt solution (melt) in the pores. Indeed, the formation of the crystalline tetrahydrate in the pores with a diameter of 15 nm and below was not observed at room temperature [19].

The liquid phase may be arranged differently in the pore space. Some of the arrangement variants are shown in Fig. 4:

—The solution is localized in narrow waists (Fig. 4a) and blocks the Knudsen diffusion of vapor through them. This lengthens the diffusion path, which is formally equivalent to an increase in the tortuosity factor for the pores in which water is transported through the vapor phase.

—The solution spreads over the surface (Fig. 4b), forming a connected cluster through which water molecules can diffuse continuously. The vapor phase also forms a connected cluster, so the diffusion fluxes through the two phases are independent and additive (see below).

—The vapor domains do not form a connected cluster and are separated by solution domains (Fig. 4c). In this case, the transport of water molecules includes their transfer across the vapor/solution interface. A similar situation takes place when solution domains are separated by vapor domains.

—The entire pore space is filled with the salt solution (Fig. 4d). In this case, water diffuses only through the liquid phase.

It is expected that, with an increasing amount of sorbed water, the gas phase transport will diminish and the liquid-phase transport will increase. Under the assumption that water is transported simultaneously over the connected clusters of the vapor and liquid phases (Fig. 4b) and that the pores have the simple shape of a cylinder (Fig. 5a), the total diffusion flux $J_\Sigma$ can be represented as the sum of the corresponding fluxes:

$$J_\Sigma = J_g + J_l = -D_g S_g \frac{dC_g}{dz} - D_l S_l \frac{dC_l}{dz}$$

$$= -\left[ D_g(S_g/S) + D_l(S_l/S)\left(\frac{dC_l}{dz}/\frac{dC_g}{dz}\right)\right] S\frac{dC_g}{dz}$$

$$= -\left[ D_g(S_g/S) + D_l(S_l/S)\frac{dC_l}{dC_g}\right] S\frac{dC_g}{dz} = -D_\Sigma S\frac{dC_g}{dz},$$

where $D_\Sigma = D_g(S_g/S) + D_l(S_l/S)\dfrac{dC_l}{dC_g} = D_g(S_g/S) + D_l(S_l/S)K$.

Here, $z$ is the coordinate along the pore (Fig. 5a), $S_g$ and $S_l$ are the mass transfer areas of the gas and liquid phases, $S$ is the total mass transfer area ($S = S_g + S_l$), $C_g$ and $C_l$ are the water concentrations in the gas and liquid phases, and $K = dC_l/dC_g$ is the local slope of the sorption isotherm (Fig. 5b). There are analytical expressions suggested for describing the additive contributions from different mechanisms of gas (water)

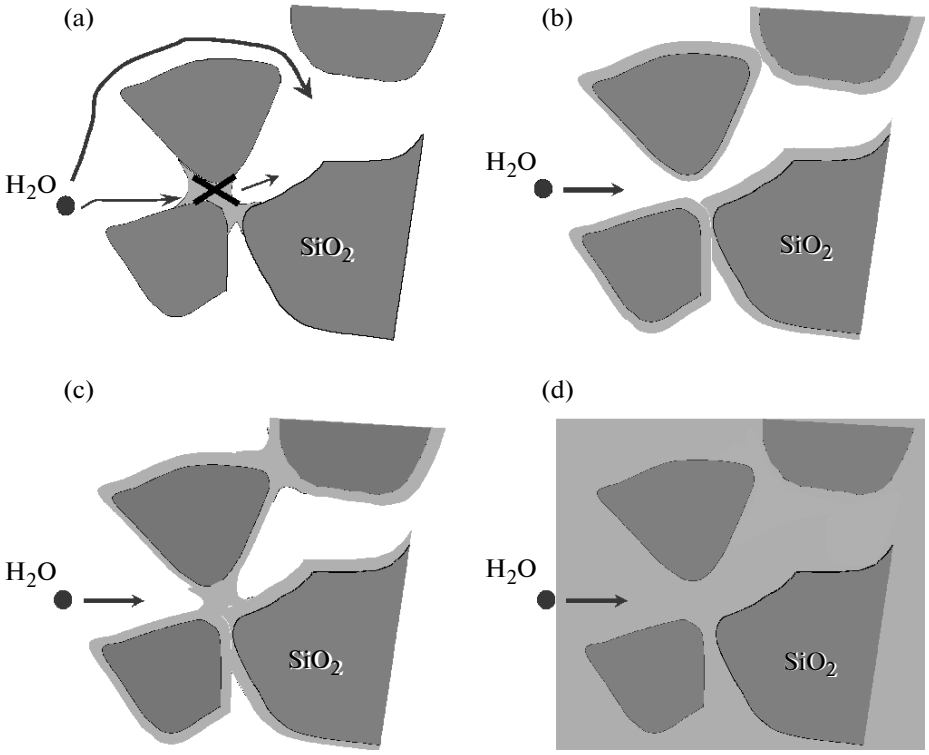


**Fig. 4.** Variants of the arrangement of the salt and its solution in matrix pores (see discussion in the main text).

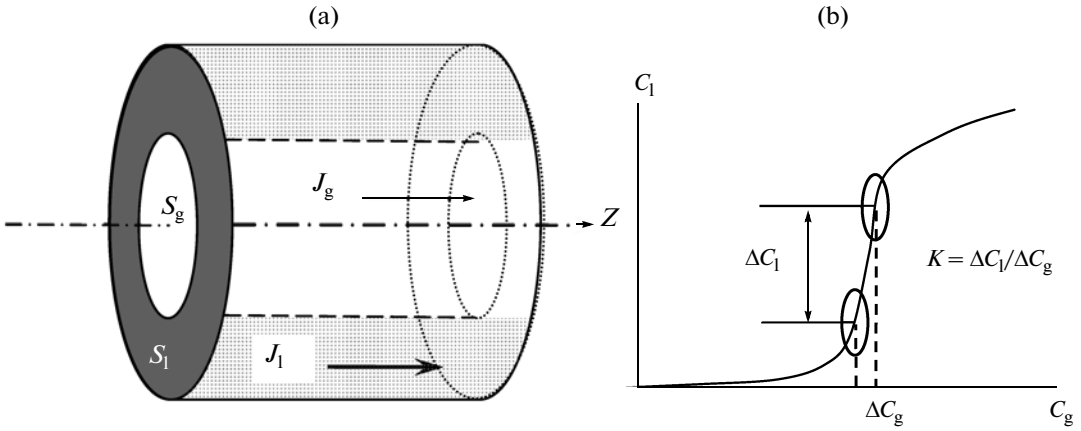


**Fig. 5.** (a) Diffusion fluxes in the gas and liquid phases and (b) determination of the coefficient $K$.

transport in the following processes: capillary osmosis and thermoosmosis [20]; film flow during the evaporation of a liquid into the atmosphere of its own vapor; simultaneous flow of a vapor, liquid, and condensate in porous media [21]; and the transport of a dissolved gas in a surface liquid film [8, 22]. It is assumed in these expressions that the fluxes depend linearly on the concentration (pressure) gradient. A similar approach was taken in the calculation of the generalized mass transfer coefficient, introduced by Lykov [23] to take into account different mechanisms of internal mass transfer. Because of the complexity of these mechanisms, the generalized mass transfer coefficient can be determined only experimentally.

Transport through the gas phase intensifies with increasing $S_l$ and $K$, and this leads to an increase in the total flux if $D_g(S_g/S) + D_l(S_l/S) > D_g$ or $D_lK > D_g$. The vapor-phase diffusivity estimated above for the Knudsen transport mechanism is $D_g = 1.8 \times 10^{-6}$ m$^2$/s. We will assume that the diffusivity of water in the aqueous solution of calcium chloride in the pores is equal to the diffusivity of water in the massive calcium chloride solution. The latter depends only slightly on the salt concentration in the 0.05–3.0 M range and is $(1.2 \pm 0.1) \times$

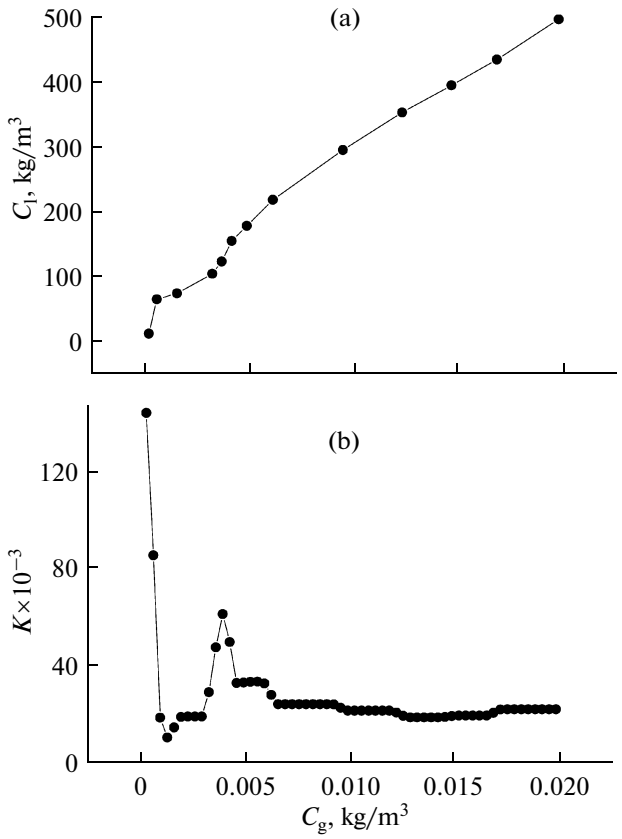


**Fig. 6.** (a) Water sorption isotherm at $T$ = 35°C; (b) numerical calculation of the coefficient $K$ from the sorption isotherm.

$10^{-9}$ m$^2$/s [24]. At $K > D_g/D_l = 1.5 \times 10^3$, the presence of the liquid phase will increase the diffusion flux. The $K$ values determined by numerical differentiation of the water sorption isotherm for the composite depend on the amount of adsorbed water and vary between $13 \times 10^3$ and $55 \times 10^3$ (see Fig. 6b, which is discussed in Appendix B); that is, the contribution from the liquid-phase diffusion should be taken into account, at least when the liquid phase in the pores forms a connected cluster. Apparently, the contribution from diffusion via this channel is much smaller than is estimated above because the actual distribution of solution and vapor domains differs significantly from the simplified model presented in Fig. 5a. It is likely that vapor domains in the pores are separated by solution domains (Fig. 4d) and this slows down water transport. In this situation, water diffusion includes transfer across the vapor–solution interface and the escape of a water molecule from the solution phase into the vapor phase requires the activation barrier to be surmounted [25]. Indeed, at large degrees of filling of the pores (e.g., $\nu = 0.75$ at $N = 14.0$), the effective diffusivity is $D_{eff} = 11.3 \times 10^{-11}$ m$^2$/s (table). With the porosity of the initial silica gel ($\varepsilon = 0.67$) and the tortuosity of its pores ($\chi = 1.2$) taken into account, this $D_{eff}$ value leads to a value of $1.4 \times 10^{-10}$ m$^2$/s for the diffusivity of water in the solution filling the pores. This value is 8.6 times smaller than the diffusivity of water in a bulk calcium chloride solution [20]. A possible cause of this difference is the increased viscosity of the solution in small pores. It was demonstrated that water films may be more viscous than bulk water [26]. Another likely cause is the above-mentioned deceleration of water transport at the vapor–solution interfaces.

Although the system examined is very complex and the vapor and liquid phase domains may be arranged in the pore space in various ways, the existence of the region of the sharpest increase in $D_{eff}$ (Fig. 3, $\nu$ = 0.41–0.58 or $N$ = 8.4–11.2) can be explained by the formation of a continuous solution phase, i.e., by passing from a continuous vapor phase cluster to a continuous liquid phase cluster (Figs. 4a, 4d). This makes water transport through the liquid film more efficient. The decrease in the sorption rate at $N$ = 12.1 and 14.0 is possibly due to the further breakup of the vapor phase cluster, which causes an increase in the interfacial area and a slowdown of water transport.

The acceleration of water transport due to the formation of a liquid film on the capillary walls, owing to which the permeability of the capillary increases by a factor of 5–6 relative to the permeability level typical of the Knudsen mechanism, shows itself as the capillary size is reduced to 100–200 nm, and this result is in good agreement with theoretical estimates [21]. Note that nearly the same acceleration of water transport was observed in this study. There is extensive evidence of the intensification of water vapor transport in porous media partially filled with water [21, 27, 28], including constructional materials [29, 30].

A kinetic analysis of isothermal water sorption by the $CaCl_2$/silica gel composite initiated by a small stepwise change in the vapor pressure over the sample at a constant plate temperature of 35°C indicates that the initial portion of the kinetic curves can be described in terms of Fick's diffusion model. At small amounts of sorbed water ($N \le 4.5$, or $w \le 0.16$ g/g), the diffusivity of water in the pores, $D$, calculated from experimental data is close to the Knudsen diffusivity for water vapor, so Knudsen diffusion is the rate-determining mechanism. As the water content of the composite is further raised, the water sorption rate increases; that is, the presence of sorbed water accelerates water transport in the composite pores. This is likely due to the appearance of an additional channel of water diffusion, namely, diffusion through the aqueous solution of the salt, whose formation on the silica gel surface begins at $w \approx 0.1$ g/g. The contribution from this channel increases appreciably when the amount of sorbed water exceeds 0.25 g/g. This can be due to the formation of a "connected" phase of the solution in the pores. As the amount of sorbed water further increases, sorption slows down. This can be due to the alternation of vapor and liquid phase domains and the appearance of the corresponding vapor–solution

interfaces, at which the diffusion rate of water molecules is lower.

With the appearance of the connected cluster of the solution, the contribution from diffusion through the liquid phase should increase at those amounts of sorbed water to which the maximum isotherm slope $K$ corresponds. Note that, when the process takes place on a salt-in-porous-matrix composite, the local isotherm slope $K$ may be as large as $10^5$, 1–2 orders of magnitude larger than for the process occurring on an unmodified porous matrix (e.g., silica gel) [8]. This is due to two circumstances: firstly, the composite sorbs 5–7 times more water; secondly, the salt introduced into the pores sorbs a large amount of water within a narrow range of water concentrations in the gas phase (Fig. 5b). Thus, water diffusion through the liquid phase plays a much more significant role in the salt-in-porous-matrix composites than it does in the host matrix.

The intensification of water transport due to water diffusion through the liquid phase may have implications for the propagation of organic pollutants and transport of gaseous hydrocarbons in moist soil [8, 22], for the operation of proton exchange membranes in fuel cells [31], for heat and moisture transport in constructional materials [29], and for adsorption and other processes in porous media partially filled with a liquid [8, 32].

## APPENDIX A

### *Analysis of Sorption Kinetic Curves*

The mass balance equation determining the kinetics of gas sorption on by identical spherical granules of an adsorbent can be written as

$$(1-\varepsilon)\frac{\partial C_l}{\partial t} + \varepsilon\frac{\partial C_g}{\partial t} = \varepsilon D\left(\frac{\partial^2 C_g}{\partial R^2} + \frac{2}{R}\frac{\partial C_g}{\partial R}\right), \qquad (A.1)$$

where $D$ is the effective coefficient of diffusion in the pores, which is assumed to be independent of the concentration of sorbed water; $t$ is the sorption time; and $R$ is the radial coordinate. When the concentration increment is small ($\Delta C_g \ll C_g^0$, where $C_g^0$ is the initial concentration of water molecules in the gas phase before the beginning of its variation), the following relationship is valid:

$$\frac{\partial C_l}{\partial t} = K\frac{\partial C_g}{\partial t}, \qquad (A.2)$$

where $K = K(C_g^0) = \text{const}$. Equation (A.1) will then appear as

$$\frac{\partial C_g}{\partial t} = \frac{\varepsilon D}{\varepsilon + (1-\varepsilon)K}\left(\frac{\partial^2 C_g}{\partial R^2} + \frac{2}{R}\frac{\partial C_g}{\partial R}\right). \qquad (A.3)$$

Here, $R$ is the spherical coordinate.

In this case, the boundary and initial conditions can be written as follows:

$$t < 0,\ C_g = C_g^0,\ C_l = C_l^0,$$
$$t \geq 0,\ C_g = C_g',\ C_l(r_c,t) = C_l(t),$$

where $C_l^0$ is the initial water concentration in the liquid phase and $C_g'$ is the concentration of water molecules in the gas phase immediately after the beginning of concentration variation, so the concentration step is $\Delta C_g = C_g' - C_g^0$.

The solution of Eq. (A.3) is as follows [9]:

$$\frac{m_t}{m_\infty} = \frac{\overline{C}_l - C_l^0}{C_l^\infty - C_l^0} = 1 - 6\sum_{n=1}^{\infty}\frac{\exp\left(-\dfrac{n^2\pi^2 D_{eff}t}{r_c^2}\right)}{9\Lambda/(1-\Lambda) + (1-\Lambda)p_n^2}, \qquad (A.4)$$

where $\overline{C}_l$ is the granule-average concentration of adsorbed water, $C_l^\infty$ is the equilibrium concentration of adsorbed water, $p_n$ is a nonzero root of the transcendent equation $\tan p_n = \dfrac{3p_n}{3 + (1/\Lambda - 1)p_n^2}$, $\Lambda = \dfrac{\Delta P_a}{\Delta P_0}$ is the adsorption-induced change in the water vapor pressure normalized to the initial pressure jump at $t = 0$, and $D_{eff} = D\dfrac{\varepsilon}{\varepsilon + (1-\varepsilon)K}$.

At small $t$ values, expression (A.3) tends to

$$\frac{m_t}{m_\infty} = \frac{1}{1-\Lambda}\frac{6}{\sqrt{\pi}}\sqrt{\frac{D_{eff}t}{r_c^2}}.$$

Thus, the effective diffusivity $D_{eff}$ can be derived from the slope of the kinetic curve in the $\dfrac{m_t}{m_\infty} - \sqrt{t}$ coordinates at small $t$ values.

## APPENDIX B

### *Calculating the diffusivity of Water in the Pores*

The diffusivity of water in a pore was calculated using the formula $D = D_{eff}\dfrac{\varepsilon + (1-\varepsilon)K}{\varepsilon}$ [9], where $K$ is the slope of the isotherm in the $C_l$–$C_g$ coordinates (Fig. 6a), $C_l$ is the adsorbate concentration in the condensed phase (kg/m$^3$), $C_g$ is the adsorptive concentration in the gas phase (kg/m$^3$), and $\varepsilon$ is the porosity of

the adsorbent granules. The concentration of sorbed water was calculated as $C_l = \frac{m_t}{m_\infty}\rho_{gr}$, where $\rho_{gr}$ is the density of the sorbent granules, which was taken to be constant (0.92 kg/m$^3$). The $K$ value was determined by numerical differentiation of the experimental water sorption isotherm (Fig. 6b).

The sorbent porosity $\varepsilon(w)$ was calculated taking into account the volume occupied by the crystalline hydrate and/or salt solution in the pores, which increases as water is sorbed:

$$\varepsilon = \frac{V_p - \frac{w+g}{(1-g)\rho}}{V_{gr}},$$

where $V_{gr}$ is the granule volume. All values here are for 1 g of the sorbent. For supersaturated solutions, we plotted the density of the solution versus the salt concentration, $\rho(g)$. To do this, we extrapolated literature data for unsaturated solutions to the supersaturated region.

## REFERENCES


1. Kel'tsev, N.V., *Osnovy adsorbtsionnoi tekhniki* (Principles of Adsorption), Moscow: Khimiya, 1984.
2. Yang, R.T., *Adsorbents: Fundamentals and Applications*, New Jersey: Wiley, 2003.
3. Alefeld, G. and Radermacher, R., *Heat Conversion Systems*, Boca Raton, Fla.: CRC, 1994.
4. Thomson, G., *The Museum Environment*, London: Butterworth-Heinemann, 1986.
5. Aristov, Yu.I., Gordeeva, L.G., and Tokarev, M.M., *Kompozitnye sorbenty "sol' v poristoi matritse": sintez, svoistva, primeneniya* (Salt-in-Porous-Matrix Composite Sorbents: Synthesis, Properties, and Applications), Novosibirsk: Sib. Otd. Ross. Akad. Nauk, 2008.
6. Aristov, Yu.I. and Gordeeva, L.G., *Kinet. Catal.*, 2009, vol. 50, p. 65.
7. Aristov, Yu.I., Tokarev, M.M., Di Marko, G., Cacciola, G., Restuccia, G., and Parmon, V.N., *Russ. J. Phys. Chem.*, 1997, vol. 71, p. 197.
8. Ho, C.K. and Webb, S.W., *Gas Transport in Porous Media*, Dordrecht: Springer, 2006.
9. Kaerger, J. and Ruthven, D.M., *Diffusion in Zeolites and Other Microporous Solids*, New York: Wiley, 1992.
10. Crank, J., *Mathematics of Diffusion*, London: Oxford Univ. Press, 1975.
11. Tunitskii, N.N., Kaminskii, V.A., and Timashev, S.F., *Metody fiziko-khimicheskoi kinetiki* (Methods of Physicochemical Kinetics), Moscow: Khimiya, 1972.
12. Aristov, Yu.I., Glaznev, I.S., Freni, A., and Restuccia, G., *Kinet. Catal.*, 2006, vol. 47, p. 770.
13. Pankrat'ev, Yu.D., Tokarev, M.M., and Aristov, Yu.I., *Russ. J. Phys. Chem.*, 2001, vol. 75, p. 806.
14. *Kirk–Othmer Encyclopedia of Chemical Technology*, New York: Wiley, 1999, vol. 4, p. 413, 4th ed.
15. Neimark, A.V., Kheifets, L.I., and Fenelonov, V.B., *Ind. Eng. Chem. Prod. Res. Dev.*, 1981, vol. 20, p. 439.
16. Aristov, Yu.I., *Katal. Prom–sti.*, 2004, no. 6, p. 36.
17. Lee, L.K. and Ruthven, D.M., *J. Chem. Soc., Faraday Trans. 1*, 1979, vol. 75, p. 2406.
18. Aristov, Yu.I., Tokarev, M.M., Freni, A., Glaznev, I.S., and Restuccia, G., *Microporous Mesoporous Mater.*, 2006, vol. 96, p. 65.
19. Tokarev, M.M., *Extended Abstract of Cand. Sci. (Chem.) Dissertation*, Novosibirsk: Inst. of Catalysis, 2003.
20. Deryagin, B.V., Churaev, N.V., and Muller, V.M., *Poverkhnostnye sily* (Surface Forces), Moscow: Nauka, 1987.
21. Churaev, N.V., *Fiziko-khimiya protsessov massoperenosa v poristykh telakh* (Physical Chemistry of Mass Transfer in Porous Bodies), Moscow.
22. Jury, W.A., Russo, D., Streile, G., and El Abd, H., *Water Resour. Res.*, 1990, vol. 26, p. 13.
23. Lykov, A.V., *Teplomassoobmen* (Heat and Mass Transfer), Moscow: Energiya, 1972.
24. Harned, H.S. and Parker, H.W., *J. Am. Chem. Soc.*, 1965, vol. 77, p. 265.
25. Valiullin, R.R., Skirda, V.D., Stapf, S., and Kimmich, R., *Phys. Rev. E: Stat. Nonlinear Soft Matter Phys.,* 1997, vol. 55, p. 2664.
26. Zorin, Z.M., Sobolev, V.D., and Churaev, N.V., *Dokl. Akad. Nauk SSSR*, 1970, vol. 93, p. 630.
27. Lykov, A.V., *Transportnye yavleniya v kapillyarno-poristykh telakh* (Transport Phenomena in Capillary Porous Bodies), Moscow: Gostekhizdat, 1954.
28. Koptyug, I.V., Khitrina, L.Yu., Aristov, Yu.I., Tokarev, M.M., Iskakov, K.T., Parmon, V.N., and Sagdeev, R.Z., *J. Phys. Chem. B*, 2000, vol. 104, p. 1695.
29. Nizovtsev, M.I., Stankus, S.V., Sterlyagov, A.N., Terekhov, V.I., and Khairulin, R.A., *Int. J. Heat Mass Transfer*, 2008, vol. 51, p. 4161.
30. Chen, Z.Q. and Shi, M.H., *Appl. Therm. Eng.*, 2005, vol. 25, p. 61.
31. Hyun Nam, J. and Kaviany, M., *Int. J. Heat Mass Transfer*, 2003, vol. 46, p. 4595.
32. Kaviany, M., *Principles of Heat Transfer in Porous Media*, New York: Springer, 1991.